



OPEN

Monomeric streptavidin phage display allows efficient immobilization of bacteriophages on magnetic particles for the capture, separation, and detection of bacteria

Caitlin M. Carmody & Sam R. Nugen

Immobilization of bacteriophages onto solid supports such as magnetic particles has demonstrated ultralow detection limits as biosensors for the separation and detection of their host bacteria. While the potential impact of magnetized phages is high, the current methods of immobilization are either weak, costly, inefficient, or laborious making them less viable for commercialization. In order to bridge this gap, we have developed a highly efficient, site-specific, and low-cost method to immobilize bacteriophages onto solid supports. While streptavidin–biotin represents an ideal conjugation method, the functionalization of magnetic particles with streptavidin requires square meters of coverage and therefore is not amenable to a low-cost assay. Here, we genetically engineered bacteriophages to allow synthesis of a monomeric streptavidin during infection of the bacterial host. The monomeric streptavidin was fused to a capsid protein (Hoc) to allow site-specific self-assembly of up to 155 fusion proteins per capsid. Biotin coated magnetic nanoparticles were functionalized with mSA-Hoc T4 phage demonstrated in an *E. coli* detection assay with a limit of detection of < 10 CFU in 100 mLs of water. This work highlights the creation of genetically modified bacteriophages with a novel capsid modification, expanding the potential for bacteriophage functionalized biotechnologies.

Bacteriophages (phages) are viruses that bind and infect specific bacterial strains. Their ability to specifically target bacteria has made them useful tools for detecting and combating their host bacteria^{1–5}. Phages have been immobilized to various materials to impart functional capabilities including antimicrobial activity^{6,7}, bacteria capture^{8,9}, and nanostructure scaffolding^{10–12}. T4 phages have been immobilized to polycaprolactone film to functionalize the film with antimicrobial activity resulting in a significant reduction of *E. coli* O157:H7 on beef when in contact with the film¹³. Filamentous phage E2 was immobilized to magnetoelastic filter elements used to capture greater than 90% of target bacteria pathogens passed through the liquid filter system¹⁴. Additionally, the repeating highly ordered structure of M13 bacteriophages have been utilized to assemble nanowires via polyelectrolyte multilayering for use in a lithium ion battery electrode¹⁵.

The phages' proteinaceous structure allows for immobilization via affinity interactions between functional groups on amino acid side chains and material surfaces. A comprehensive collection of phage immobilization strategies can be found in recent reviews^{16,17}. For most applications, phages need to be immobilized by their negatively charged capsids to allow proper orientation of the positively charged tail fibers. The tail fibers are responsible for binding bacteria and triggering infection, outward towards the sample. Silica^{18,19}, cellulose^{20,21}, gold^{18,22,23}, and carbon^{1,24} materials have been functionalized with positively charged compounds or polymers to allow immobilization of phages via their capsid. Charge-oriented phages immobilized to chemically functionalized gold have been shown to have higher phage depositing density and bacteria capturing capacity when compared to non-functionalized controls^{25,26}. The process of chemically functionalizing materials typically requires toxic organic solvents, complex reactor setups, and expensive equipment^{27–29}. Additionally, the effectiveness of charge-based immobilization is often dependent on the ion concentration of the sample matrix.

Department of Food Science, Cornell University, Ithaca, NY 14853, USA. email: snugen@cornell.edu

Alternatively, phages can be genetically modified for site-specific immobilization. A gene for a protein affinity tag fused to a phage capsid protein gene can be incorporated into phage genomes or expressed exogenously from a plasmid to create a capsid modified phage. This well-established “Phage Display” method is frequently used to study protein–protein interactions for pharmaceutical applications^{30–32} and has been employed to immobilize phages to cellulose and streptavidin supports^{33–36}. CRISPR/Cas9, can be used to help expedite the editing and selection process for genomic modification of phages^{37–39}. This system is composed of a guide RNA (gRNA) which can be designed to target a specific DNA sequence and an endonuclease (Cas9) responsible for double stranded DNA cleavage of the target. This double strand DNA cleavage activates genomic repair pathways which can facilitate of incorporation of new DNA into the genome via homologous recombination⁴⁰. This method has been used in previous work on the same phage and capsid gene that was modified in this study to achieve > 99% recombinant phages produced⁴¹.

If bacteriophages are to be immobilized on magnetic particles for the capture and separation of bacteria, the avidity between the phage and particle must allow for the pulling of a relatively larger bacterium. Streptavidin-modified particles have often been used for separation following binding of a biotinylated recognition element. While the kd of streptavidin–biotin is known to be $\approx 10^{-5}$ nM, the purified protein is relatively expensive. In the case of magnetic nanoparticles, the required surface functionalization could be several m².⁴² For the system to have commercial viability, the conjugation method must be cost-effective and scalable.

We hypothesize that a specific, stable, and high affinity monomeric version of streptavidin (mSA)⁴³ can be displayed on the surface of bacteriophages using genetic engineering. In this study, the gene for mSA was fused to the highly antigenic outer capsid protein (Hoc) gene in a T4 phage genome to generate a novel capsid modified phage capable of oriented immobilization to biotin coated materials. This allows the more expensive constituent in the streptavidin–biotin system to be synthesized during the infection of host bacteria. The mSA-Hoc then self-assembles on the phage capsid during viral assembly. A luciferase gene carrying variant of the well-characterized, *E. coli* infecting T4 phage was selected for this study due to previous success with genetic modifications⁴¹ and ability for small and large foreign proteins to be displayed on the capsid while maintaining infectivity^{34,44–47}. The functionality of mSA-Hoc was assessed via phage immobilization onto biotin coated magnetic nanoparticles. The ability of the phage-magnetic particle system was demonstrated in a detection assay for *E. coli* from water with a limit of detection of < 10 CFU/100 mLs. The improved conjugation method and demonstrated performance represent a step forward for commercialization of magnetic phage-based sensors for capture, separation, and detection of their host bacteria. This novel phage capsid modification can be extended to other phages to allow for site-specific immobilization to the plethora of widely available biotinylated materials, expanding potential of phage-based detection, biocontrol, and biomedicine technologies.

Materials and methods

Bacteria, phage, and plasmids

E. coli NEB® 5-alpha chemically competent cells were used for cloning and obtained from NEB (Ipswich, MA, USA). *E. coli* (ECOR #13), a strain isolated from a healthy human, was obtained from the Thomas S. Whittam STEC Center (East Lansing, MI, USA). *E. coli* DH5α and wild type T4 phages were obtained from ATTC (Manassas, VA USA). T4 phages containing NanoLuc:CBM luciferase reporter (NRGP17) were engineered in a previous study⁴¹. Addgene plasmids pCRISPR (#42875) and pCas9 (#42876) were gifts from Luciano Marraffini⁴⁸. Addgene plasmid pRSET-*msa* (#39860) was a gift from Sheldon Park.⁴³ Bacteria overnight cultures were grown shaking 90 rpm at 37 °C overnight in Luria–Bertani (LB) broth with appropriate antibiotic supplementation (50 µg/mL Kanamycin for pCRISPR, 25 µg/mL Chloramphenicol for pCas9). Phage propagation via liquid lysate was carried out as described by Bonilla et al.⁴⁹. Phages were initially purified by centrifugation at 3260 × g for 30 min to remove cell debris followed by filtration through a 0.2 µm cellulose nitrate or cellulose acetate vacuum filter system from Corning (Corning, NY, USA) to remove NanoLuc:CBM background. Phages were concentrated via centrifugation (25,000 × g, 3 h, 4 °C) and resuspension in a 0.5 mL of SM buffer. Concentrated phages were incubated with 6 mm cellulose fiber discs from Whatman (Florham Park, NJ, USA) overnight to further remove NanoLuc:CBM background. Phage enumeration via double layer plaque assay was used to determine Plaque Forming Units (PFU).

Materials and reagents

All cloning reagents were purchased from New England Biolabs (Ipswich, MA, USA). Nano-Glo luminescent reagent was purchased from Promega (Madison, WI, USA) and prepared immediately before use according to the manufacturer’s recommendations. Luminescent signals were monitored using a Synergy Neo 2 Hybrid Multimode Reader (Biotek Instruments, Winooski, VT, USA). Ninety-six well filter plates (0.2 µm PVDF) were purchased from Corning (Corning, NY, USA). Multi-well plate manifold for filtering 96-well plates was purchased from Pall (Cortland, NY, USA). All other reagents were purchased from Thermo Fisher Scientific (Waltham, MA, USA). Primers are listed in Table S1.

Donor plasmid construction

The guide RNAs (gRNA) used to target *hoc* were designed in Geneious Prime (Biomatters, Ltd., Auckland, NZ) and ordered from IDT as single stranded DNA oligos (Coralville, IA, USA). The gRNA were cloned into pCRISPR (a gRNA expression plasmid for targeting a specific sequence) following Marraffini’s protocol⁴⁸. The donor DNA expression cassette consisting of a chimeric monomer of streptavidin and rhizavidin (mSA) optimized for high-affinity binding biotin⁴³, T4 phage *hoc* codon optimized to be resistant to the gRNA used in this study, and regions of homology to T4 phage *hoc* were synthesized via PCR amplification using pRSET-*msa* and T4 phage genomic DNA as templates (Fig. S2). The donor DNA expression cassette constituents and gRNA containing

pCRISPR were ligated together via Gibson assembly cloning⁵⁰ following the NEBuilder Hifi DNA Assembly manufacture protocol. The donor plasmid sequence was confirmed via colony PCR in-house followed by Sanger sequencing performed by the Biotechnology Resource Center (BRC) Genomics Facility (RRID:SCR_021727) at Cornell Institute of Biotechnology (Ithaca, NY, USA) using Applied Biosystems Automated 3730xl DNA Analyzers, Big Dye Terminator chemistry, and AmpliTaq FSDNA Polymerase.

Recombinant phage construction

CRISPR/Cas9 mediated engineering was used to construct recombinant phages as previously described⁴¹. The system relies on a gRNA designed to target a specific DNA sequence and an endonuclease to generate a double strand DNA break in the target sequence. In the base phage NRGP17, there was a nonsense mutation in hoc approximately 1000 bp away from the site of the desired mSA addition. The distance between these two sites was too large to simultaneously edit both areas at once. Two separate engineering steps were needed with different gRNA for the two modifications. Phage genomes were edited using a modified protocol from Duong et. al.⁴¹. The phage with the repaired hoc nonsense mutation was named NRGP28. The phage with the mSA-modified Hoc was named NRGP56.

Creating T4 Recombinants. *E. coli* NEB 5-alpha cells containing pCRISPR (gRNA + donor sequence) and pCas9 were added to 0.8% LB top agar containing the appropriate antibiotics and mixed. Then 100 μ L of 106 PFU/ml NRGP17 phages were added to the same tube containing molten agar, mixed, and poured onto an LB plate. Plates were incubated overnight at 37 °C.

Background removal

A spot over assay was done via plaque transfer to minimize endogenous background from the donor plasmid containing *E. coli*. Overnight culture (200 μ L) of *E. coli* DH5a without any plasmids was added to molten 0.8% LB top agar, mixed, and poured onto a gridline square LB plate. A sterile toothpick was used to transfer plaques resulting from the previous day's plaque assay over to the gridline square spot assay plate. Plates were incubated overnight at 37 °C (Supplementary Figure S1).

Screening for T4 recombinants

PCR was performed on the plaques following Novagen's T7Select System's plaque PCR protocol (Madison, WI, USA). A single plaque PCR confirmed positive phage was propagated, genomes were extracted from lysate using Norgen Phage DNA Isolation Kit (Norgen Biotek Corporation, Canada), and whole genome sequenced performed by the Cornell university College of Veterinary Medicine Animal Health Diagnostic Center, Department of Molecular Diagnostics (Ithaca, NY, USA) via Illumina mySeq platform and Illumina Basespace Sequence Hub for data acquisition and quality control analysis. All sequencing data were analyzed in Geneious Prime® (Biomatters, Ltd., Auckland, NZ).

Immobilization of phages to biotin coated magnetic nanoparticles

The mSA-Hoc phages were partially pre-blocked with biotin at room temperature for 40 min to help limit crosslinking of the beads using a ratio of 10 biotin molecules to 1 mSA-Hoc protein. Magnetic biotin coated nanoparticles from Raybiotech (Peachtree Corners, GA, USA) were removed from their storage solution and prepared according to the manufacturer's manual with a modification to the wash buffer (TTBS with 0.5% tween 20 and biotin). Pre-blocked phages (3.5×10^7 PFU) were added to prepared beads and incubated with rotation for 5 min at room temperature. A magnetic stand was used to separate the nanoparticles from the supernatant. Nanoparticles were washed twice with 1 mL wash buffer before final resuspension in 500 μ L of wash buffer and stored at 4 °C.

Detection of *E. coli* in 10 ml

The procedure for detection of *E. coli* in small volume samples (10 mL) has been described previously⁵¹. Single colonies of *E. coli* (ECOR#13) were grown shaking for 16–18 h in 10 mL of LB broth. Serial dilutions were performed in Phosphate Buffered Saline (PBS). Bacteria were enumerated using standard plate-counting to determine Colony Forming Units (CFU/mL). Samples (10 mL) of autoclaved tap water (Cornell University water supply) were spiked with either 100 μ L 10^{-7} *E. coli* dilution (66–124 CFU), 100 μ L of the 10^{-8} *E. coli* dilution (3–16 CFU), or 100 μ L of PBS. The *E. coli* concentrations of the final inoculum was confirmed using standard plate counts performed in technical triplicate for each biological replicate. A total of 500 μ L of $20 \times$ LB broth was added to each sample and were incubated with shaking 200 rpm at 37 °C for 3 h. Phage bead supernatant was removed and replaced with an equivalent volume of LB immediately before use in the detection assay. A total of 250 μ L of phage immobilized particles was added to each sample and incubated shaking 90 rpm for 10 min. Samples were poured into square Petri dishes to maximize the surface area and placed against a magnetic rig (magnetic bars adhered to 10 cm² supports). Supernatants were aspirated and discarded followed by particle resuspension in 500 μ L of LB broth. Resuspended beads were incubated shaking (90 rpm) for 3 h at 37 °C followed by filtration through 96-well filter plates with a 6 mm cellulose fiber disk added to each well to capture the Nanoluc:CBM. A 50 μ L aliquot of NanoGlo reagent was added to each well and let incubate at room temperature for 10 min before reading luminescence. The detection assay was performed using three biological replicates. The Limit of Detection (LOD) was determined using the 0 + 3SD method where the lowest positive signal is defined as the values of the negative control + three standard deviations^{52–55}.

Detection of *E. coli* in 100 ml

Based on previously described protocol⁵¹, *E. coli* (ECOR#13) preparation and dilution were the same as described above. Bacteria were enumerated using standard plate-counting to determine Colony Forming Units (CFU). Samples (100 mL) of autoclaved tap water were spiked with either 100 μ L of 10^{-7} *E. coli* dilution (81 ± 24 CFU), 100 μ L of 10^{-8} *E. coli* dilution (9 ± 4 CFU), or 100 μ L of PBS (Negative control). Each sample received 5 mL of $20 \times$ LB broth for resuscitation followed by incubation with shaking (200 rpm at 37 °C for 3 h). Phage bead supernatant was removed and replaced with an equivalent volume of LB immediately before use in the detection assay. A total of 500 μ L of phage immobilized particles was added to each sample and incubated shaking 90 rpm for 10 min. Samples were poured into square Petri dishes to maximize the surface area and placed against a magnetic rig (magnetic bars adhered to 10 cm² supports). Supernatants were aspirated and discarded followed by particle resuspension in 500 μ L of LB broth. Resuspended beads were incubated shaking 90 rpm for an additional 3 h at 37 °C followed by filtration, luminescent detection, LOD determination as described above. The detection assay was performed in three biological replicates.

Results and discussion

Genetic engineering of bacteriophages

The genetic engineering tool, CRISPR/Cas9, was used to translationally fuse a monomer streptavidin affinity tag (mSA) to the nonessential highly antigenic outer capsid protein (hoc) of T4 bacteriophage. The overall genetic engineering process is depicted in Fig. 1. A donor plasmid was synthesized via Gibson Assembly cloning⁵⁰ to incorporate the donor DNA fragment composed of mSA-hoc codon optimized to be resistant to the gRNA targeting hoc flanked by homologous arms (~1500 bp). The N-terminus of Hoc was selected for mSA fusion due to previous studies demonstrating improved capsid binding of Hoc N-terminal fusion proteins when compared to C-terminus fusion proteins, due to the C-terminus of Hoc containing the T4 capsid protein binding domain^{47,56,57}. Large homologous arm lengths were chosen because it has been reported that increasing homologous arm length can increase recombination rate^{37,58}. Within the bacteria cell, the CRISPR effector complex facilitated the recombination of wild type T4 phage with the donor DNA to produce recombinant mSA-hoc phage progeny (NRGP56). Phage genomic incorporation of mSA was confirmed via Sanger and whole genome sequencing (Supplementary Information 2) of plaques.

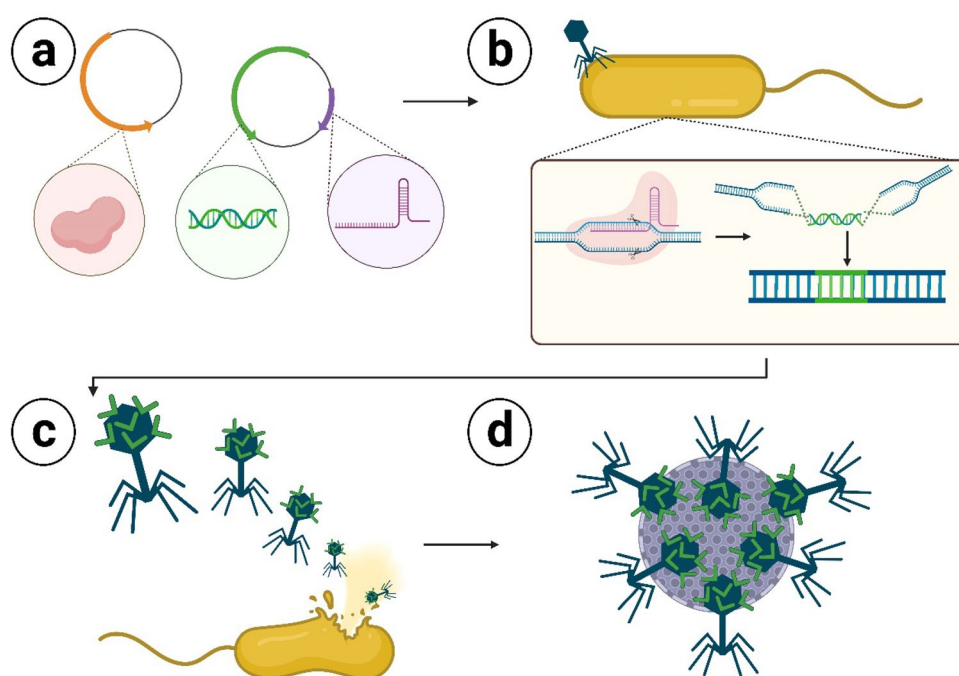


Figure 1. CRISPR/Cas9 genetic engineering of bacteriophages workflow. (a) Two plasmids encode all components for forming a CRISPR effector complex able to identify and cleave the targeted DNA sequence in the phage genome. One plasmid also delivers the donor DNA sequence composed of the desired DNA to be incorporated into the phage genome flanked by regions of homology to the phage genome cleavage site. (b) Wild type bacteriophages infect a bacteria cell containing the plasmids encoding the CRISPR effector complex components and donor DNA. The phage genome is cleaved by the CRISPR effector complex. The cleaved phage genome repairs itself with the donor DNA sequence via homologous recombination. (c) Recombinant phage progeny are released from the bacteria cell at the end of the lytic replication cycle. (d) Recombinant phages have improved functional capabilities for numerous biotechnology applications.

Immobilization of engineered bacteriophages

The NRGP56 phages were immobilized to biotin coated magnetic nanoparticles to assess the ability of the mSA affinity tag to facilitate immobilization. While the concentrations of modified Hoc was not sufficient for an ELISA or Western blots, when the mSA-modified NRGP56 phages were mixed with the biotin-modified magnetic particles, significant crosslinking between phages and particles resulted in the aggregation and settling of the phage-particle mass, a phenomenon not observed with the NRGP28 phages (Fig. 2). To mitigate crosslinking of nanoparticles seen during early phage immobilization phages were initially incubated with free biotin to block some of the available biotin binding sites. Then NRGP56 phages were incubated with biotin coated magnetic nanoparticles with a diameter of 500 nm alongside NRGP28 (wild type Hoc) phages as a control. The phage bead solutions were washed with wash buffer to remove unbound phages. Titering of the washes revealed the majority of the NRGP56 and NRGP28 phages remained immobilized on the beads (data not shown). The control phages remaining on the beads is likely due to weak electrostatic adsorption, which can be affected by changes in ionic strength, temperature, shear force, and pH^{59–61}. Therefore, this interaction may not be sufficient for keeping phages immobilized in some applications. To test the practical significance of modifying Hoc for immobilization, NRGP56 and NRGP28 phages immobilized to nanoparticles were compared in an *E. coli* detection assay.

E. coli detection assays

The assay workflow for target bacteria resuscitation, separation, concentration, and detection using NRGP56 and NRGP28 phages immobilized to magnetic nanoparticles is depicted in Fig. 3. The assay was initially conducted on ECOR13, an *E. coli* environmental isolate used in previous detection assays^{62,63}, in a 10 mL water sample. Standard plate counts of the inoculated water samples were performed alongside the phage-based detection assay for comparison. The assay's signal increased proportionally with ECOR13 concentration. The assay resulted in a 4.68 ± 1.82 signal:noise for 10 ± 4 CFU and 23.85 ± 13.11 signal:noise for 89 ± 19 CFU as seen in Fig. 4. The limit of detection (LOD) for ECOR13 in 10 mL of water using the NRGP56 phage assay was calculated to be approximately 1 CFU/10 mL.

To assess real world applications, the NRGP56 phage assay was scaled-up to be used on 100 mL water samples as required by the United States Environmental Protection Agency for drinking water. The assay's signal increase remained proportional with *E. coli* ECOR13 concentration. The assay resulted in a 2.83 ± 0.47 signal:noise for 9 ± 3 CFU and 13.50 ± 7.87 signal:noise for 98 ± 17 CFU as seen in Fig. 5. The limit of detection (LOD) for *E. coli* ECOR13 in 100 mL of water using the NRGP56 phage assay was calculated to be approximately 5 CFU/100 mL.

During immobilization of phages to the magnetic nanoparticles' assays described above, results indicated majority of the NRGP28 control phages were remaining immobilized to the particles even after washing. To determine if wild type Hoc alone is sufficient to provide stable immobilization that can be maintained during practical use, an NRGP28 phage detection assay was performed in 100 mL water samples. The assay's signal change was not proportional with ECOR13 concentration change. As can be seen in Fig. 5, all the variable ECOR13 concentrations had slightly lower signal:noise than the 0 CFU control. The limit of detection (LOD) for ECOR13 in 100 mL of water using the NRGP28 phage assay was calculated to be 9×10^6 CFU.

A one-way ANOVA was performed within each of the 3 trials on the 3 means of the varying *E. coli* concentrations. The NRGP56 phage detection assays produced extremely sensitive LODs (~ 1 and ~ 5 CFU for 10 and 100 mL, respectively), with significance against the control (Fig. S1). The poor performance of the NRGP28 phage detection assay suggests that the electrostatic adsorption interactions that were able to immobilize NRGP28



Figure 2. Crosslinked NRGP56 phage nanoparticles. Tubes contained the same titer of NRGP56 (left) or NRGP28 (right) phages incubated rotating for one hour on a circular rotator at room temperature. Left tube contains NRGP56 phages that resulted in nanoparticle crosslinking of the particles and loss of suspension. The black arrow indicates the aggregated phage/nanoparticles. The right tube contains NRGP28 phages with no indication of crosslinking or loss of suspension.

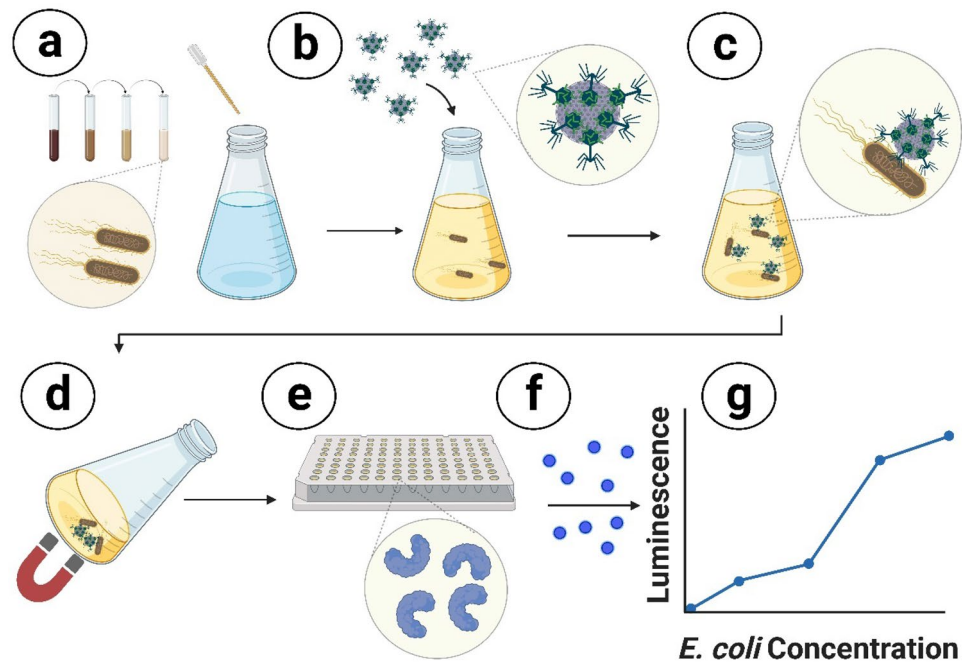


Figure 3. Bacteriophage-based *E. coli* detection assay workflow. (a) Sterile tap water samples were spiked with varying concentrations of *E. coli* and incubated shaking at 37 °C for 3 h to resuscitate cultures. (b) Bacteriophage immobilized to magnetic nanoparticles were added to the sample and incubated shaking for 10 min at 37 °C. (c) *E. coli* cells in the sample were captured by the bacteriophage immobilized nanoparticles. (d) A magnet was used to concentrate the bacteria-bacteriophage nanoparticle complex allowing the supernatant removal. (e) After 3 h of incubation (shaking at 37 °C) to allow for luciferase reporter enzyme expression and bacteria lysis to occur, samples were filtered through a 96 well filter plate to capture the luciferase reporter enzyme. (f) Luciferase substrate was added to each well and incubated at room temperature for 10 min for reaction to occur. (g) Luminescent signal was read in a spectrophotometer.

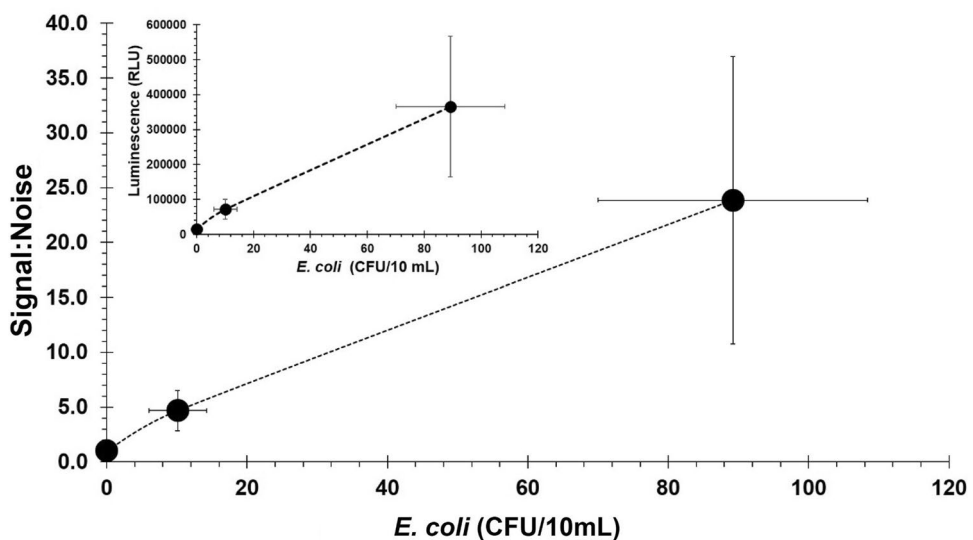


Figure 4. *E. coli* detection assay in 10 mL of water. Use of NRG56 phage particles for separation and detection of varying concentrations of *E. coli* spiked in 10 mL sterile tap water samples. Error bars represent standard deviations from biological triplicates.

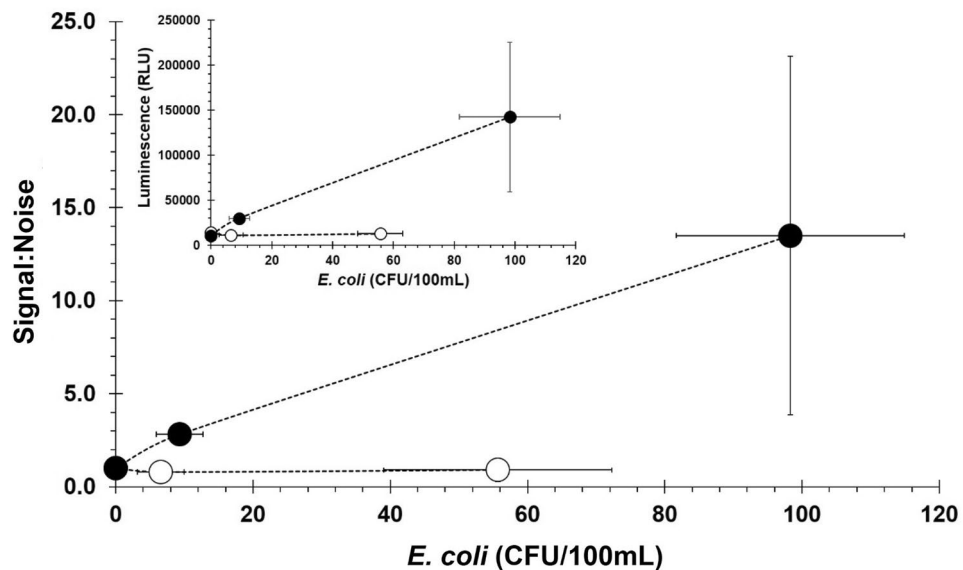


Figure 5. *E. coli* detection assay in 100 mL of water. Comparison of NRG56 phage particles (●) to NRG28 phage particles (○) for separation and detection of varying concentrations of *E. coli* spiked in 100 mL sterile tap water samples. Error bars represent standard deviations from biological triplicates.

phages to the particles are not strong enough to keep the phages immobilized during functional use in our detection assay. This could be due to the binding of the phage to the bacteria being a stronger interaction than the electrostatic adsorption to the particles. During the T4 phage infection, phage short tail fibers bind irreversibly to their receptors on the bacteria's outer membrane and phage tail tube components fuse with the bacteria's cytoplasmic membrane⁶⁴. When the magnet separated the particles from the matrix to concentrate the target bacteria, the phages were likely left behind on the bacteria instead of remaining attached to both the particles and bacteria. This suggests the necessity of the mSA modification to Hoc for the execution of this sensitive bacteria detection assay.

Conclusions

This work highlights a method to efficiently conjugate bacteriophages to biotinylated surfaces using a commercially scalable and low-cost method. The genetically modified phages with a novel monomeric streptavidin capsid modification allowed for targeted immobilization to biotin functionalized particles.

While previous reported methods have chemically modified phages to biotin for conjugation to streptavidin-modified surfaces^{65–68}, we report a method which results in mSA modified phages during propagation. The mSA has a reported K_d of 2.8 nM⁴³ and approximately 155 are displayed per phage capsid in a repeating pattern. Functionalization of phages via targeting of primary amines or carboxylic acids can result in loss of phage infectivity due to inadvertent conjugation to proteinaceous tail fibers.

Other functionalization methods include sodium periodate oxidation then oxime formation⁶⁹ and diazo linkage then copper catalyzed azide-alkyne cycloaddition⁷⁰. These reactions can also react with non-target exposed compatible functional groups, risking unintentional modification of phage components that can interfere with proper phage function. More site-specific chemical conjugation methods relying on an initial genetic unnatural amino acid incorporation have been used to modify phages with biotin^{71–74} but suffer from the complexity and inefficiency of the unnatural amino acid incorporation process^{75,76}. Phages have been genetically modified with biotin carboxyl carrier proteins, but this requires an extra step for the proteins to be biotinylated by a biotin ligase enzyme within the system for phage production^{36,77–80}. Additionally, this would require streptavidin modification of the immobilization surface which reduces commercial viability due to the cost. In our study, once the initial site-specific genomic modification was performed, the NRG56 can be propagated using the same machinery, methods, and workflows as wild type phages allowing for an overall low-cost modification. To our knowledge, this is the first phage genetically modified to express a monomeric streptavidin on its capsid.

Data availability

The datasets generated/ analyzed as well as biological samples synthesized during the current study are available from the corresponding author (snugen@cornell.edu) on reasonable request.

Received: 21 February 2023; Accepted: 12 September 2023

Published online: 27 September 2023

References

- Zhou, Y., Marar, A., Kner, P. & Ramasamy, R. P. Charge-directed immobilization of bacteriophage on nanostructured electrode for whole-cell electrochemical biosensors. *Anal. Chem.* <https://doi.org/10.1021/acs.analchem.6b03751> (2017).
- Bhardwaj, N., Bhardwaj, S. K., Mehta, J., Mohanta, G. C. & Deep, A. Bacteriophage immobilized graphene electrodes for impedimetric sensing of bacteria (*Staphylococcus arlettae*). *Anal. Biochem.* <https://doi.org/10.1016/j.ab.2016.04.008> (2016).
- Tlili, C. *et al.* Bacteria screening, viability, and confirmation assays using bacteriophage-impedimetric/loop-mediated isothermal amplification dual-response biosensors. *Anal. Chem.* <https://doi.org/10.1021/ac302699x> (2013).
- Nakama, K., Sedki, M. & Mulchandani, A. Label-free chemiresistor biosensor based on reduced graphene oxide and M13 bacteriophage for detection of coliforms. *Anal. Chem. Acta* <https://doi.org/10.1016/j.aca.2021.338232> (2021).
- Bhardwaj, N., Bhardwaj, S. K., Mehta, J., Kim, K. H. & Deep, A. MOF-bacteriophage biosensor for highly sensitive and specific detection of *Staphylococcus aureus*. *ACS Appl. Mater. Interfaces* <https://doi.org/10.1021/acsami.7b07818> (2017).
- Wang, Z., Wang, D., Kinchla, A. J., Sela, D. A. & Nugen, S. R. Rapid screening of waterborne pathogens using phage-mediated separation coupled with real-time PCR detection. *Anal. Bioanal. Chem.* <https://doi.org/10.1007/s00216-016-9511-2> (2016).
- Nogueira, F. *et al.* Immobilization of bacteriophage in wound-dressing. *Nanostruct. Nanomed. Nanotechnol. Biol. Med.* <https://doi.org/10.1016/j.nano.2017.08.008> (2017).
- Singh, A. *et al.* Immobilization of bacteriophages on gold surfaces for the specific capture of pathogens. *Biosens. Bioelectron.* <https://doi.org/10.1016/j.bios.2009.05.028> (2009).
- Naidoo, R. *et al.* Surface-immobilization of chromatographically purified bacteriophages for the optimized capture of bacteria. *Bacteriophage* <https://doi.org/10.4161/bact.19079> (2012).
- Lee, J. H. *et al.* Production of tunable nanomaterials using hierarchically assembled bacteriophages. *Nat. Protoc.* <https://doi.org/10.1038/nprot.2017.085> (2017).
- Lee, B. Y. *et al.* Virus-based piezoelectric energy generation. *Nat. Nanotechnol.* <https://doi.org/10.1038/nnano.2012.69> (2012).
- Muzard, J., Platt, M. & Lee, G. U. M13 bacteriophage-activated superparamagnetic beads for affinity separation. *Small* <https://doi.org/10.1002/sml.201200099> (2012).
- Choi, I., Yoo, D. S., Chang, Y., Kim, S. Y. & Han, J. Polycaprolactone film functionalized with bacteriophage T4 promotes antibacterial activity of food packaging toward *Escherichia coli*. *Food Chem.* **346**, 128883. <https://doi.org/10.1016/j.foodchem.2020.128883> (2021).
- Du, S. *et al.* 3D phage-based biomolecular filter for effective high throughput capture of *Salmonella typhimurium* in liquid streams. *Food Res. Int.* <https://doi.org/10.1016/j.foodres.2021.110181> (2021).
- Nam, K. T. *et al.* Virus-enabled synthesis and assembly of nanowires for lithium ion battery electrodes. *Science* <https://doi.org/10.1126/science.1122716> (2006).
- Carmody, C. M., Goddard, J. M. & Nugen, S. R. Bacteriophage capsid modification by genetic and chemical methods. *Bioconj. Chem.* <https://doi.org/10.1021/acs.bioconjchem.1c00018> (2021).
- O'Connell, L., Marcoux, P. R. & Roupioz, Y. Strategies for surface immobilization of whole bacteriophages: A review. *ACS Biomater. Sci. Eng.* <https://doi.org/10.1021/acsbiomaterials.1c00013> (2021).
- Cademartiri, R. *et al.* Immobilization of bacteriophages on modified silica particles. *Biomaterials* <https://doi.org/10.1016/j.biomaterials.2009.11.029> (2010).
- Handa, H. *et al.* Recognition of salmonella typhimurium by immobilized phage P22 monolayers. *Surf. Sci.* <https://doi.org/10.1016/j.susc.2008.01.036> (2008).
- Farooq, U. *et al.* High-density phage particles immobilization in surface-modified bacterial cellulose for ultra-sensitive and selective electrochemical detection of *Staphylococcus aureus*. *Biosens. Bioelectron.* <https://doi.org/10.1016/j.bios.2020.112163> (2020).
- Vonasek, E., Lu, P., Hsieh, Y. L. & Nitin, N. Bacteriophages immobilized on electrospun cellulose microfibers by non-specific adsorption, protein-ligand binding, and electrostatic interactions. *Cellulose* <https://doi.org/10.1007/s10570-017-1442-3> (2017).
- Rippa, M. *et al.* Octupolar metastructures for a highly sensitive, rapid, and reproducible phage-based detection of bacterial pathogens by surface-enhanced Raman scattering. *ACS Sens.* <https://doi.org/10.1021/acssensors.7b00195> (2017).
- Arya, S. K. *et al.* Chemically immobilized T4-bacteriophage for specific *Escherichia coli* detection using surface plasmon resonance. *Analyst* <https://doi.org/10.1039/c0an00697a> (2011).
- Jabrane, T., Dube, M., & Mangin, P. J. Bacteriophage immobilization on paper surface: effect of cationic pre-coat layer. In *Proceedings of Canadian PAPTAC 95th Annual Meeting* (2009).
- Xu, J., Zhao, C., Chau, Y. & Lee, Y. K. The synergy of chemical immobilization and electrical orientation of T4 bacteriophage on a micro electrochemical sensor for low-level viable bacteria detection via differential pulse voltammetry. *Biosens. Bioelectron.* <https://doi.org/10.1016/j.bios.2019.111914> (2020).
- Richter, I. *et al.* Dense layer of bacteriophages ordered in alternating electric field and immobilized by surface chemical modification as sensing element for bacteria detection. *ACS Appl. Mater. Interfaces* <https://doi.org/10.1021/acsami.7b03497> (2017).
- Woehrl, G. H., Brown, L. O. & Hutchison, J. E. Thiol-functionalized, 1.5-Nm gold nanoparticles through ligand exchange reactions: Scope and mechanism of ligand exchange. *J. Am. Chem. Soc.* <https://doi.org/10.1021/ja0457718> (2005).
- Visintin, P. M., Carbonell, R. G., Schauer, C. K. & DeSimone, J. M. Chemical functionalization of silica and alumina particles for dispersion in carbon dioxide. *Langmuir* <https://doi.org/10.1021/la047823c> (2005).
- Ellebracht, N. C. & Jones, C. W. Amine functionalization of cellulose nanocrystals for acid-base organocatalysis: Surface chemistry, cross-linking, and solvent effects. *Cellulose* <https://doi.org/10.1007/s10570-018-2043-5> (2018).
- Smith, G. P. & Petrenko, V. A. Phage display. *Chem. Rev.* <https://doi.org/10.1021/cr960065d> (1997).
- Bazan, J., Calkosiński, I. & Gamian, A. Phage display—A powerful technique for immunotherapy. *Hum. Vaccin. Immunother.* <https://doi.org/10.4161/hv.21703> (2012).
- Tan, Y., Tian, T., Liu, W., Zhu, Z. & Yang, C. Advance in phage display technology for bioanalysis. *Biotechnol. J.* <https://doi.org/10.1002/biot.201500458> (2016).
- Tong, Z. *et al.* Efficient affinity-tagging of M13 phage capsid protein ix for immobilization of protein III-displayed oligopeptide probes on abiotic platforms. *Appl. Microbiol. Biotechnol.* <https://doi.org/10.1007/s00253-019-10338-8> (2020).
- Minikh, O., Tolba, M., Brovko, L. Y. & Griffiths, M. W. Bacteriophage-based biosorbents coupled with bioluminescent ATP assay for rapid concentration and detection of *Escherichia coli*. *J. Microbiol. Methods* <https://doi.org/10.1016/j.mimet.2010.05.013> (2010).
- Tolba, M., Minikh, O., Brovko, L. Y., Evoy, S. & Griffiths, M. W. Oriented immobilization of bacteriophages for biosensor applications. *Appl. Environ. Microbiol.* <https://doi.org/10.1128/AEM.02294-09> (2010).
- Gervais, L. *et al.* Immobilization of biotinylated bacteriophages on biosensor surfaces. *Sens. Actuat. B Chem.* <https://doi.org/10.1016/j.snb.2007.03.007> (2007).
- Tao, P., Wu, X., Tang, W. C., Zhu, J. & Rao, V. Engineering of bacteriophage T4 genome using CRISPR-Cas9. *ACS Synth. Biol.* <https://doi.org/10.1021/acssynbio.7b00179> (2017).
- Martel, B. & Moineau, S. CRISPR-Cas: An efficient tool for genome engineering of virulent bacteriophages. *Nucleic Acids Res.* <https://doi.org/10.1093/nar/gku628> (2014).
- Shen, J., Zhou, J., Chen, G.-Q. & Xiu, Z.-L. Efficient genome engineering of a virulent *Klebsiella* bacteriophage using CRISPR-Cas9. *J. Virol.* <https://doi.org/10.1128/jvi.00534-18> (2018).
- Ran, F. A. *et al.* Genome engineering using the CRISPR-Cas9 system. *Nat. Protoc.* <https://doi.org/10.1038/nprot.2013.143> (2013).

41. Duong, M. M., Carmody, C. M., Qinqin, M., Peters, J. E. & Nugen, S. R. Optimization of T4 phage engineering via CRISPR/Cas9. *Sci. Rep.* **10**(1), 18229 (2020).
42. Avvakumova, S., Colombo, M., Galbiati, E., Mazzucchelli, S., Rotem, R., Prosperi, D. Bioengineered approaches for site orientation of peptide-based ligands of nanomaterials. In *Biomedical Applications of Functionalized Nanomaterials: Concepts, Development and Clinical Translation* 139–169 (2018). <https://doi.org/10.1016/B978-0-323-50878-0.00006-9>
43. Lim, K. H., Huang, H., Pralle, A. & Park, S. Stable, high-affinity streptavidin monomer for protein labeling and monovalent biotin detection. *Biotechnol. Bioeng.* <https://doi.org/10.1002/bit.24605> (2013).
44. Tao, P., Li, Q., Shivachandra, S. B. & Rao, V. B. Bacteriophage T4 as a nanoparticle platform to display and deliver pathogen antigens: Construction of an effective anthrax vaccine. *Methods Mol. Biol.* https://doi.org/10.1007/978-1-4939-6869-5_15 (2017).
45. Sathaliyawala, T. *et al.* Assembly of human immunodeficiency virus (HIV) antigens on bacteriophage T4: A novel in vitro approach to construct multicomponent HIV vaccines. *J. Virol.* <https://doi.org/10.1128/jvi.00235-06> (2006).
46. Li, Q., Shivachandra, S. B., Leppla, S. H. & Rao, V. B. Bacteriophage T4 capsid: A unique platform for efficient surface assembly of macromolecular complexes. *J. Mol. Biol.* <https://doi.org/10.1016/j.jmb.2006.08.049> (2006).
47. Ceglarek, I. *et al.* A novel approach for separating bacteriophages from other bacteriophages using affinity chromatography and phage display. *Sci. Rep.* <https://doi.org/10.1038/srep03220> (2013).
48. Jiang, W., Bikard, D., Cox, D., Zhang, F. & Marraffini, L. A. RNA-guided editing of bacterial genomes using CRISPR-Cas systems. *Nat. Biotechnol.* <https://doi.org/10.1038/nbt.2508> (2013).
49. Bonilla, N. & Barr, J. J. Phage on tap: A quick and efficient protocol for the preparation of bacteriophage laboratory stocks. *Methods Mol. Biol.* https://doi.org/10.1007/978-1-4939-8682-8_4 (2018).
50. Gibson, D. G. *et al.* Enzymatic assembly of DNA molecules up to several hundred kilobases. *Nat. Methods* <https://doi.org/10.1038/nmeth.1318> (2009).
51. Zurier, S., Duong, M., Goddard, M. & Nugen, R. Engineering biorthogonal phage-based nanobots for ultrasensitive, in situ bacteria detection. *ACS Appl. Bio Mater.* <https://doi.org/10.1021/acsabm.0c00546> (2020).
52. Missler, U., Wiesmann, M., Friedrich, C. & Kaps, M. S-100 protein and neuron-specific enolase concentrations in blood as indicators of infarction volume and prognosis in acute ischemic stroke. *Stroke* <https://doi.org/10.1161/01.STR.28.10.1956> (1997).
53. Kessler, M. A. Determination of copper at ng ml⁻¹-levels based on quenching of the europium chelate luminescence. *Anal. Chim. Acta* [https://doi.org/10.1016/S0003-2670\(98\)00152-4](https://doi.org/10.1016/S0003-2670(98)00152-4) (1998).
54. Kjems, L. L. *et al.* Highly sensitive enzyme immunoassay of proinsulin immunoreactivity with use of two monoclonal antibodies. *Clin. Chem.* <https://doi.org/10.1093/clinchem/39.10.2146> (1993).
55. Hinkley, T. C. *et al.* Reporter bacteriophage T7NLC utilizes a novel Nanoluc::CBM fusion for the ultrasensitive detection of: *Escherichia coli* in water. *Analyst* <https://doi.org/10.1039/c8an00781k> (2018).
56. Sathaliyawala, T. *et al.* Functional analysis of the highly antigenic outer capsid protein, hoc, a virus decoration protein from T4-like bacteriophages. *Mol. Microbiol.* <https://doi.org/10.1111/j.1365-2958.2010.07219.x> (2010).
57. Shivachandra, S. B. *et al.* Multicomponent anthrax toxin display and delivery using bacteriophage T4. *Vaccine* <https://doi.org/10.1016/j.vaccine.2006.10.010> (2007).
58. Dong, J. *et al.* Engineering T4 bacteriophage for in vivo display by type v CRISPR-cas genome editing. *ACS Synth. Biol.* <https://doi.org/10.1021/acssynbio.1c00251> (2021).
59. Archer, M. J. & Liu, J. L. Bacteriophage T4 nanoparticles as materials in sensor applications: Variables that influence their organization and assembly on surfaces. *Sensors* <https://doi.org/10.3390/s90806298> (2009).
60. Nap, R. J., Božič, A. L., Szleifer, I. & Podgornik, R. The role of solution conditions in the bacteriophage Pp7 capsid charge regulation. *Biophys. J.* <https://doi.org/10.1016/j.bpj.2014.08.032> (2014).
61. Hosseinioust, Z., Olsson, A. L. J. & Tufenkji, N. Going viral: Designing bioactive surfaces with bacteriophage. *Colloids Surf. B Biointerfaces* <https://doi.org/10.1016/j.colsurfb.2014.05.036> (2014).
62. Zurier, H. S., Duong, M. M., Goddard, J. M. & Nugen, S. R. Engineering biorthogonal phage-based nanobots for ultrasensitive, situ bacteria detection. *ACS Nano* <https://doi.org/10.1021/acsabm.0c00546> (2020).
63. Hinkley, T. C. *et al.* A phage-based assay for the rapid, quantitative, and single CFU visualization of *E. coli* (ECOR #13) in drinking water. *Sci. Rep.* <https://doi.org/10.1038/s41598-018-33097-4> (2018).
64. Hu, B., Margolin, W., Molineux, I. J. & Liu, J. Structural remodeling of bacteriophage T4 and host membranes during infection initiation. *Proc. Natl. Acad. Sci. U. S. A.* <https://doi.org/10.1073/pnas.1501064112> (2015).
65. Huang, L. *et al.* Labeling and single-particle-tracking-based entry mechanism study of vaccinia virus from the tiantan strain. *Anal. Chem.* <https://doi.org/10.1021/acs.analchem.7b05183> (2018).
66. Zhao, X. *et al.* Labeling of enveloped virus via metabolic incorporation of azido sugars. *Bioconjug. Chem.* <https://doi.org/10.1021/acs.bioconjchem.5b00310> (2015).
67. Abello, N., Kerstjens, H. A. M., Postma, D. S. & Bischoff, R. Selective acylation of primary amines in peptides and proteins. *J. Proteome Res.* <https://doi.org/10.1021/pr070154e> (2007).
68. Sun, W., Brovko, L. & Griffiths, M. Use of bioluminescent salmonella for assessing the efficiency of constructed phage-based biosorbent. *J. Ind. Microbiol. Biotechnol.* <https://doi.org/10.1038/sj.jim.7000198> (2001).
69. Ng, S., Jafari, M. R., Matochko, W. L. & Derda, R. Quantitative synthesis of genetically encoded glycopeptide libraries displayed on M13 phage. *ACS Chem. Biol.* <https://doi.org/10.1021/cb300187t> (2012).
70. Li, K. *et al.* Chemical modification of M13 bacteriophage and its application in cancer cell imaging. *Bioconjug. Chem.* <https://doi.org/10.1021/bc900405q> (2010).
71. Kang, S. *et al.* Implementation of P22 viral capsids as nanoplatfroms. *Biomacromol* <https://doi.org/10.1021/bm100877q> (2010).
72. Larocca, D., Witte, A., Johnson, W., Pierce, G. F. & Baird, A. Targeting bacteriophage to mammalian cell surface receptors for gene delivery. *Hum. Gene Ther.* <https://doi.org/10.1089/hum.1998.9.16-2393> (1998).
73. Saleh, L., Noren, C. J. Chapter 9. Site-Directed Chemical Modification of Phage Particles (2011). <https://doi.org/10.1039/9781847559920-00202>
74. Sandman, K. E., Banner, J. S. & Noren, C. J. Phage display of selenopeptides [6]. *J. Am. Chem. Soc.* <https://doi.org/10.1021/ja992462m> (2000).
75. Ryu, Y. & Schultz, P. G. Efficient incorporation of unnatural amino acids into proteins in *Escherichia coli*. *Nat. Methods* <https://doi.org/10.1038/nmeth864> (2006).
76. Smolskaya, S., Zhang, Z. J. & Alfonta, L. Enhanced yield of recombinant proteins with site-specifically incorporated unnatural amino acids using a cell-free expression system. *PLoS ONE* <https://doi.org/10.1371/journal.pone.0068363> (2013).
77. Kadiri, V. M. *et al.* Genetically modified M13 bacteriophage nanonets for enzyme catalysis and recovery. *Catalysts* <https://doi.org/10.3390/catal9090723> (2019).
78. Chen, J. *et al.* Bacteriophage-based nanoprobe for rapid bacteria separation. *Nanoscale* <https://doi.org/10.1039/c5nr03779d> (2015).
79. Edgar, R. *et al.* High-sensitivity bacterial detection using biotin-tagged phage and quantum-dot nanocomplexes. *Proc. Natl. Acad. Sci. U. S. A.* <https://doi.org/10.1073/pnas.0601211103> (2006).
80. Wang, Z., Wang, D., Chen, J., Sela, D. A. & Nugen, S. R. Development of a novel bacteriophage based biomagnetic separation method as an aid for sensitive detection of viable *Escherichia coli*. *Analyst* <https://doi.org/10.1039/c5an01769f> (2016).

Acknowledgements

This work is supported in part by the National Institute of Biomedical Imaging and Bioengineering (NIBIB) R01EB027895 and NIFA Hatch (NYC-143416, NYC-143802). This work was also supported by USDA NIFFA predoctoral fellowships 2020-09959.

Author contributions

C.M.C.: Conceptualization, Methodology, Investigation, Validation, Data Curation, Writing—Original Draft, Writing—Review & Editing. S.R.N.: Conceptualization, Writing—Review & Editing, Project administration, Supervision, Funding acquisition.

Competing interests

The authors declare no competing interests.

Additional information

Supplementary Information The online version contains supplementary material available at <https://doi.org/10.1038/s41598-023-42626-9>.

Correspondence and requests for materials should be addressed to S.R.N.

Reprints and permissions information is available at www.nature.com/reprints.

Publisher's note Springer Nature remains neutral with regard to jurisdictional claims in published maps and institutional affiliations.



Open Access This article is licensed under a Creative Commons Attribution 4.0 International License, which permits use, sharing, adaptation, distribution and reproduction in any medium or format, as long as you give appropriate credit to the original author(s) and the source, provide a link to the Creative Commons licence, and indicate if changes were made. The images or other third party material in this article are included in the article's Creative Commons licence, unless indicated otherwise in a credit line to the material. If material is not included in the article's Creative Commons licence and your intended use is not permitted by statutory regulation or exceeds the permitted use, you will need to obtain permission directly from the copyright holder. To view a copy of this licence, visit <http://creativecommons.org/licenses/by/4.0/>.

© The Author(s) 2023